

fastMI: a fast and consistent copula-based nonparametric estimator of mutual information

Soumik Purkayastha^a, Peter X.K. Song^{a,*}

^aDepartment of Biostatistics, University of Michigan, Ann Arbor, MI 48109, USA.

Abstract

As a fundamental concept in information theory, mutual information (MI) has been commonly applied to quantify association between random variables. Most existing estimators of MI have unstable statistical performance since they involve parameter tuning. We develop a consistent and powerful estimator, called fastMI, that does not incur any parameter tuning. Based on a copula formulation, fastMI estimates MI by leveraging Fast Fourier transform-based estimation of the underlying density. Extensive simulation studies reveal that fastMI outperforms state-of-the-art estimators with improved estimation accuracy and reduced run time for large data sets. fastMI provides a powerful test for independence that exhibits satisfactory type I error control. Anticipating that it will be a powerful tool in estimating mutual information in a broad range of data, we develop an R package fastMI for broader dissemination.

Keywords: copula, kernel density estimation, Fast Fourier transformation, data-splitting inference, statistical dependence,

2020 MSC: Primary 62H12, Secondary 62G05

1. Introduction

Investigating dependence between two random variables is a key issue in statistical science. Classical measures like Pearson's r , Kendall's τ , and Spearman's ρ [7] serve as effective measures for linear (Pearson's r) or non-linear but monotonic association (Kendall's τ and Spearman's ρ), but are incapable of detecting a non-linear, non-monotonic association that cannot be properly estimated using ranks. More sophisticated measures, like the distance correlation (dCor) [29], the Heller-Heller-Gorfine (HHG) [10] statistic and the maximal information coefficient (MIC) [22] have been introduced to study more complex

*Corresponding author. Email address: pxsong@umich.edu

association patterns. These statistics demonstrate good theoretical properties as well as stable numerical performance. Among many non-linear association metrics, mutual information (MI) [3] has recently re-emerged in statistics and machine learning literature with many exciting applications [32]. Originally introduced in a communication theory context [25], MI is a remarkably general and intuitive measure of dependence. Its widespread use in practice is due in part to the self-equitability [13] of MI - the ability to characterize dependency strength for both linear and non-linear relationships between arbitrary random variables.

For continuous data, which shall be the focus of this paper, there are three distinct MI estimation approaches. The first approach implements a binning method to group continuous data into different bins and estimates MI from the binned data [20, 28]. Success of this naive method depends heavily on proper specification of both the number, as well as the position of said bins. Another approach is based on a k-nearest neighbors (kNN) estimation method, utilized by the Kraskov-Stögbauer-Grassberger (KSG) estimator [14]. As is the case with all kNN-based methods, the KSG estimator heavily depends on properly specifying the number of neighbors. The third approach is based on estimates of probability density functions, using histograms, kernel density estimation (KDE) [18], B-splines [6], or wavelets [21]. This nonparametric approach relies on a bandwidth parameter that needs to be tuned in the estimation.

Although the approaches mentioned above demonstrate good numerical properties [6, 14, 18, 20, 21], they are highly sensitive to proper specification of tuning parameter(s). As a consequence, the resulting estimators may be unstable and/or suffer from serious bias. A recent study [35] presents a bandwidth-free KDE approach to estimate MI in which the bandwidth parameter is automatically set to maximise the jackknifed version of MI (henceforth referred to as JMI). Not only does this method exhibit greater estimation efficiency than other existing MI estimation approaches but it also provides a stable hypothesis test for independence that is shown to be more powerful than its competitors such as the dCor, HHG, or MIC. According to existing literature, JMI serves as the current gold-standard for estimating MI as well as is the choice of test for independence [35].

Along the line of bandwidth-free estimation, an improvement on JMI is proposed in this paper. This estimator is motivated by the self-consistent density estimator proposed by [1, 19] in order to minimise the mean integrated squared error (MISE) between the estimated density and the true density without incurring any manual parameter tuning. Utilizing this “optimal” density estimator, we propose a plug-in estimator of MI, termed as the *fastMI*, which is shown to be consistent and manyfold faster than the original JMI

for large data sets. This new `fastMI` automatically determines the bandwidth by minimising the MISE objective function in a data-adaptive way.

Simulation studies comparing estimation accuracy reveal `fastMI` outperforms the gold standard JMI estimator. We compare the empirical power of `fastMI` with JMI when testing for independence and note a superior performance of `fastMI`, especially in the scenarios of small sample sizes. We report a significant improvement in computation time of `fastMI` over JMI as well, in particular in the cases of large data sets. Through extensive numerical experiments, `fastMI` demonstrates improved estimation efficiency, higher empirical power when testing for independence and reduced computation time.

The rest of the paper is organized as follows. In [section 2](#) we define MI and underline a key connection of MI with copula. In [section 3](#) we describe the self-consistent density estimation method in greater detail. This section also provides theoretical guarantees on the asymptotic behaviour of the `fastMI` estimator. We present extensive simulation studies in [section 4](#) to highlight the strengths and advantages of using `fastMI` over the existing state-of-the-art estimator, the JMI estimator. Finally, we present an application of `fastMI` to real data in [section 5](#) before summarizing our findings in the concluding [section 6](#).

2. Methods

2.1. Mutual information and its copula-based formulation

Consider two continuous random variables X and Y whose joint probability density function (PDF) is denoted by f_{XY} . Mutual information (MI) is defined as

$$MI(X, Y) = \mathbb{E} \left[\log \left\{ \frac{f_{XY}(X, Y)}{f_X(X)f_Y(Y)} \right\} \right],$$

where f_X and f_Y are the marginal PDFs associated with X and Y respectively. It is known that MI is a true measure of association; that is, it is equal to zero if and only if X and Y are independent and positive otherwise. Larger values of MI indicate stronger association. MI is invariant under monotonic transformations, which is an important property allowing various rank-based estimation methods. Further, MI satisfies the self-equitability condition [35], implying that it detects associations without a bias for specific association patterns, unlike MIC [13].

Interestingly, MI may be rewritten as a function of copulas, a primary class of dependence models. From Sklar's theorem [5], we note that a bivariate PDF can be expressed in terms of an underlying copula

density function and the product of the marginal densities as follows:

$$c_{XY}(u_X, u_Y) = \frac{f_{XY}\{F_X^{-1}(u_X), F_Y^{-1}(u_Y)\}}{f_X\{F_X^{-1}(u_X)\}f_Y\{F_Y^{-1}(u_Y)\}}, \quad (1)$$

where $(u_X, u_Y)^T = \{F_X(X), F_Y(Y)\}^T$, F_X and F_Y are the cumulative distribution functions (CDFs) associated with X and Y , while F_X^{-1} and F_Y^{-1} are the corresponding quantile functions. Using Equation 1, we can rewrite MI as the negative of the entropy of the copula density [16] of the following form:

$$MI(X, Y) = -h(c) = \int_{[0,1]^2} c(u_X, u_Y) \log \{c(u_X, u_Y)\} du_X du_Y. \quad (2)$$

This expression in (2) frees the computation of MI from the marginal distributions and removes the need for faithfully capturing their properties in the estimation procedure. Thus, MI may be estimated by plugging in a copula estimator. Such a copula-based estimation approach separate the relevant entropy from the irrelevant entropies, thereby reducing potential estimation errors for better analytic and numerical performances. The separation of the copula from the marginals makes copula-based estimation methods robust to any marginal irregularity, in contrast with a direct estimation based on density dependent methods, such as the kNN-based KSG estimator, where estimating marginal densities is needed in order to estimate MI. Recognizing MI as an integral in Equation 2, we may invoke a certain data generative methodology, such as the classical Monte Carlo methods [23] for estimation purposes. In effect, the copula density function c is the target unknown to be estimated, followed by hypothesis testing, which is the focus of this paper.

2.2. Nonparametric estimation of copulas

Our nonparametric estimation method of the copula c_{XY} given in Equation 1 can be used to model any general dependency structure and does not involve making assumptions on the structure of data [26]. One challenge in using nonparametric copula estimators is due to the closed support of the copula: the support of a bivariate copula is restricted to the unit square $[0, 1]^2$. Most kernel estimators, for instance, have problems with such bounded support because for points close to the boundaries, they typically place some positive mass outside of the support. To address this, we apply a transformation such that the support of the density in the transformed space is unbounded [24]. We wish to estimate the copula density c_{XY} in Equation 1 given data $(u_X, u_Y)^T$. Let Φ be the standard normal CDF and ϕ be the standard normal PDF. We invoke an inverse-normal (or probit) transformation, where the transformed random variables $(v_X, v_Y)^T = \{\Phi^{-1}(u_X), \Phi^{-1}(u_Y)\}^T$

have normally distributed marginals with joint density f , given by:

$$f(v_X, v_Y) = c_{XY} \{\Phi(v_X), \Phi(v_Y)\} \phi(v_X) \phi(v_Y),$$

which, after change of variables, is given by

$$c_{XY}(u_X, u_Y) = \frac{f\{\Phi^{-1}(u_X), \Phi^{-1}(u_Y)\}}{\phi\{\Phi^{-1}(u_X)\} \phi\{\Phi^{-1}(u_Y)\}}, \quad (3)$$

where f is the unspecified density function that will be estimated nonparametrically. According to [24], in the probit-transformed domain, nonparametric estimation works well and has reduced asymptotic and boundary problems since the density slowly converges to zero on the edges. In section 3 we provide details and theoretical guarantees that yield the fastMI estimator.

2.3. Nonparametric estimation of fastMI

Having obtained a consistent estimator \hat{f} (see section 3), we compute our plug-in estimator fastMI estimator using Equation 2 and Equation 3, given by

$$\widehat{MI}_{fast} = n^{-1} \sum_{j=1}^n \log \left[\hat{c}_{XY} \left\{ \hat{F}_X(X_j), \hat{F}_Y(Y_j) \right\} \right], \quad (4)$$

where \hat{F}_X and \hat{F}_Y are the empirical CDFs of X and Y respectively.

Being an attractive alternative to the KDE-based estimation, our proposed method invokes fast Fourier transformation to greatly improve computational speed. In addition, our proposed estimators also have desirable large-sample properties. The density estimator so obtained, is called the *self-consistent estimator* (SCE), which is then applied to estimate MI and establish statistical inference for dependence. Consequently, we name the SCE-based MI estimator fastMI. Our SCE-based approach presents an appealing solution for objectively and optimally choosing both the kernel shape and bandwidth [1, 19] that is unencumbered by the need for user-selected parameters or tuning.

Kernel density estimators (KDEs) are commonly used for estimating PDFs. A well-known technical challenge in the KDE method is to determine a kind of optimal bandwidth H in addition to a specifically chosen kernel density. Albeit a vast literature on this issue of bandwidth tuning, selecting optimal H remains case-dependent and computationally burdensome, and oftentimes this task involves directly a manual user-intervention [26]. A review of automatic selection methods [9] recommends a variety of different ap-

proaches that are dependent on data set characteristics (including sample size, smoothness, and skewness) and thus is hard to implement in practise. While some bandwidth-free KDEs such as JMI are used in the estimation of MI, the resulting estimators are not obtained by minimising MSEs. Such a drawback is illustrated in simulation studies in [section 4](#) and overcome by our proposed PDF estimation method.

3. Self-consistent Density Estimation

3.1. Formulation

Let us consider a random bivariate sample denoted by $\mathcal{S} = \{\mathbf{Z}_j = (X_j, Y_j) \in \mathcal{X} \times \mathcal{Y}, j = 1, 2, \dots, n\}$ from density f , which belongs to the Hilbert space of square integrable functions, given by

$$\mathcal{L}^2 = \left\{ f : \int f^2(\mathbf{z})d\mathbf{z} < \infty \right\}.$$

Without loss of generality, we assume $\mathcal{X} \times \mathcal{Y} = \mathbb{R}^2$. We consider the SCE $\hat{f} \in \mathcal{L}^2$. In order to define \hat{f} , we require a kernel function K , which belongs to the class of functions given by

$$\mathcal{K} := \left\{ K : K(\mathbf{z}) \geq 0 \forall \mathbf{z}; K(\mathbf{z}) = K(-\mathbf{z}) \forall \mathbf{z}; \int K(\mathbf{z})d\mathbf{z} = 1 \right\}.$$

Specifically, \hat{f} is given by the convolution of a kernel K and the set of delta functions centered on the dataset as follows:

$$\begin{aligned} \hat{f}(\mathbf{z}) &:= n^{-1} \sum_{j=1}^n K(\mathbf{z} - \mathbf{Z}_j), \mathbf{z} \in \mathbb{R}^2 \\ &= n^{-1} \sum_{j=1}^n \int_{\mathbb{R}^2} K(\mathbf{t})\delta(\mathbf{z} - \mathbf{Z}_j - \mathbf{t})d\mathbf{t}, \end{aligned} \tag{5}$$

where $\delta(\mathbf{z})$ is the Dirac delta function [15]. Our aim is identify the optimal kernel \hat{K} , where ‘‘optimal’’ is intended as minimising the mean integrated square error (MISE) between the true density f and the estimator \hat{f} :

$$\begin{aligned} \hat{K} &:= \operatorname{argmin}_{K \in \mathcal{K}} \text{MISE}(\hat{f}, f) \\ &= \operatorname{argmin}_{K \in \mathcal{K}} \mathbb{E} \left[\int_{\mathbb{R}^2} \{\hat{f}(\mathbf{z}) - f(\mathbf{z})\}^2 d\mathbf{z} \right], \end{aligned} \tag{6}$$

where the \mathbb{E} operator denotes taking expectation over the entire support of f . Of note, the above optimal kernel is obtained by a data-driven machinery with no need of bandwidth selection. The SCE in [Equation 5](#)

may be represented equivalently by its inverse Fourier transform pair, $\hat{\phi} \in \mathcal{L}^2$:

$$\hat{\phi}(\mathbf{t}) = \mathcal{F}^{-1}(\hat{f}(\mathbf{z})) = \kappa(\mathbf{t})C(\mathbf{t}), \quad (7)$$

where \mathcal{F}^{-1} represents the multidimensional inverse Fourier transformation from space of data $\mathbf{z} \in \mathbb{R}^2$ to frequency space coordinates $\mathbf{t} \in \mathbb{R}^2$. $\kappa = \mathcal{F}^{-1}(K)$ is the inverse Fourier transform of the kernel K and C is the empirical characteristic function (ECF) of the data, defined as

$$C(\mathbf{t}) = n^{-1} \sum_{j=1}^{n_1} \exp(it' \mathbf{Z}_j). \quad (8)$$

The optimal transform kernel $\hat{\kappa}$ that minimizes the MISE in Equation 6 is as follows [1, 19]

$$\hat{\kappa}(\mathbf{t}) = \frac{n}{2(n-1)} \left[1 + \sqrt{1 - \frac{4(n-1)}{|nC(\mathbf{t})|^2}} \right] I_{A_n}(\mathbf{t}). \quad (9)$$

Note that A_n serves as a low-pass Fourier filter that yields a stable estimator. We follow standard nomenclature [1] and denote A_n as the set of ‘‘acceptable frequencies’’. For further discussion on A_n please see Section 1.3 of the Supplement.

The optimal transform kernel $\hat{\kappa}$ in Equation 9 may be anti-transformed back to the real space to obtain the optimal kernel \hat{K} , which also belongs to \mathcal{K} . The classical kernel estimation approach [26] assumes a specific form (such as the Gaussian kernel or Epanechnikov kernel) of the kernel K_H which depends on a bandwidth parameter H and requires tuning H according to some optimality criterion, like minimum MISE. In contrast, the SCE method makes minimal assumptions on the functional form of K , and its estimate \hat{K} is determined entirely by a data-driven approach.

3.2. Theoretical guarantees

We now present key large-sample properties for the SCE estimator and the subsequent plug-in estimator of MI, beginning with Theorem 1 that establishes strong consistency of the SCE estimator \hat{f} at all points on the support of f .

Theorem 1. *Let the true density f be square integrable and its corresponding Fourier transform ϕ be integrable, then the self consistent estimator \hat{f} , which is defined by Equation 5 - Equation 9 converges almost surely to f as $n \rightarrow \infty$, under the additional assumptions $\mathcal{V}(A_n) \rightarrow \infty$, $\mathcal{V}(A_n)/\sqrt{n} \rightarrow 0$ and*

$\mathcal{V}(\bar{A}_n) \rightarrow 0$ as $n \rightarrow \infty$. Further, assuming f to be continuous on support \mathbb{R}^2 , we have uniform almost sure convergence of \hat{f} to f as $n \rightarrow \infty$.

Proof: Here A_n represents the frequency filter that ensures a stable solution of the SCE \hat{f} . \bar{A}_n is the complement of A_n and the volume of A_n is given by $\mathcal{V}(A_n)$. The proof of [Theorem 3](#) is given in Section S.1.4 of the Supplement.

The estimator \widehat{MI}_{fast} so obtained is consistent, as established by [Theorem 2](#) below.

Theorem 2. *Let the assumptions of [Theorem 1](#) hold. Further, we assume the true underlying copula function c_{XY} is bounded away from zero and infinity on its support. Then, the estimator \widehat{MI}_{fast} given by [Equation 4](#) converges in probability to the true MI as $n \rightarrow \infty$.*

Proof: The proof of [Theorem 2](#) is given in Section S.2.1 of the Supplement.

On the basis of [Theorem 2](#), we can propose a permutation-based test for independence, i.e., a test for $H_0 : MI = 0$ against the alternative $H_a : MI > 0$.

3.3. Test for independence

The estimator \widehat{MI}_{fast} may be used to test for independence between X and Y . Rejection rules of the test based on asymptotic theory require data with large sample sizes, which may not be always available in practice. To ensure a stable and reliable performance, we implement a permutation-based test as it can give a precise finite-sample distribution of the test statistic for even small samples [17]. For a random sample of n observations, $S = \{(X_j, Y_j)\}_{j=1}^n$, let $\{\delta(1), \delta(2), \dots, \delta(n)\}$ be a random permutation of $\{1, 2, \dots, n\}$. Based on δ -permuted data set $S_\delta = \{(X_j, Y_{\delta(j)})\}_{j=1}^n$, we calculate the corresponding estimate \widehat{MI}_{fast} . On repeating the above procedure r times, $\mathcal{T}_{perm} = \left\{ \widehat{MI}_{fast}^{\delta_r} \right\}_{r=1}^R$, a collection of estimates is obtained, which may be used to approximate the null distribution of \widehat{MI}_{fast} , under the null hypothesis $H_0 : X$ and Y are independent. At significance level α , we reject the null hypothesis when \widehat{MI}_{fast} based on the original data is greater than the $(1 - \alpha)$ th empirical quantile of \mathcal{T}_{perm} .

4. Simulation studies

4.1. Estimation accuracy of MI

In this section, we compare the efficiency of the fastMI estimator with that of the existing gold-standard estimator of MI, the JMI. Previous simulation studies [35] show that the JMI has the smallest mean-squared

error (MSE) for a wide class of multivariate association patterns across different sample sizes, thereby indicating its superior performance. Through extensive simulation studies, we compare the MSE performance of `fastMI` with JMI for a wide range of bivariate association patterns, for different sample sizes. We generate a sample of n observations drawn from a bivariate PDF f_{XY} on \mathbb{R}^2 , specified by the underlying copula and marginal densities. Since marginal densities do not play a role in determining underlying mutual information, we fix them to be standard normal densities across all models for convenience.

We restrict ourselves to three separate classes of copula models [5, 11] - the symmetric Gaussian copula and two asymmetric Archimedean copula - the Clayton and Gumbel copula. While the Clayton copula exhibits greater dependence in the negative tail, the Gumbel copula exhibits greater dependence in the positive tail. Each of these copula classes may be specified by fixing the underlying value of Kendall's τ , which in turn, may be used to compute the underlying true MI [2]. For each of the three copula classes considered, we fix $\tau \in \{0, 0.1, 0.2, \dots, 0.9\}$ and generate $n \in \{100, 250, 500\}$ bivariate samples. The simulated data are used to compute both JMI and `fastMI`. The MSEs of both estimators for different models and sample sizes are calculated based on $r = 1000$ replications. Our findings are presented in Figure 1. We note that `fastMI` has appreciably lower MSE for all models and sample sizes considered, indicating its superior performance over JMI.

4.2. Test for independence

We compare the permutation-based tests proposed for both `fastMI` and JMI. For the same bivariate patterns as described in subsection 4.1, with $\tau \in \{0, 0.05, \dots, 0.50\}$ ($\tau = 0$ indicates independence), we plot the empirical power curves for the tests at significance level $\alpha = 0.05$ and present our results in Figure 2. We note that `fastMI` rejects the null hypothesis of independence with higher empirical power than JMI even for moderate sample sizes. This is an appreciable improvement over the current gold-standard JMI, where, with modest amounts of data, nonparametric estimation may be a sufficiently challenging task [27]. For increased sample sizes, both methods show similar empirical power. Overall, `fastMI` demonstrates a more stable and more powerful test of independence when compared to JMI.

Previous replicable studies [35] have compared the performance of the JMI-based test with other popular methods, including `dCor`, `HHG` and `MIC`-based tests, and concluded that JMI appears to be the most stable test for independence. Given that in almost all the simulation settings `fastMI` clearly outperform JMI, our proposed nonparametric estimator is found to be a fast, efficient and reliable method of choice to estimate MI and to conduct a hypothesis test for independence with high power while exhibiting type I error control.

4.3. Computation time

Since nonparametrically estimating MI is a computationally intensive method, we compare run times of both `fastMI` and `JMI` for various sample sizes for bivariate data. We report the mean and standard deviation of run time in [Table 1](#). Of note, for smaller sample sizes, `JMI` is faster and has a lower run time than `fastMI`; in contrast, as sample size increases, `fastMI` becomes fast with run times being many fold smaller than `JMI`. This improvement in run time establishes `fastMI` as an attractive method for studying association in practice, because it is the case of large sample size that matters in real-world computations.

	$n = 250$	$n = 500$	$n = 1000$	$n = 2500$	$n = 5000$
JMI	0.112 (0.02)	0.688 (0.045)	2.969 (0.179)	18.073 (1.663)	71.938 (4.076)
<code>fastMI</code>	0.313 (0.115)	0.760 (0.284)	2.481 (1.141)	9.389 (1.814)	20.387 (0.269)

Table 1: Mean (standard deviation) computation time of `JMI` and `fastMI` (in seconds) for bivariate data of varying sample size (n).

5. Real data analysis

As an application of our method to real data, we study the dependence between $X =$ “death rate” and $Y =$ “birth rate” in 229 countries and territories around the world in the first trimester of 2020 [8]. (X, Y) denote the number of deaths and births per year per 1000 individuals in the country. [Figure 3](#) presents a scatterplot of this data, with each point on the plot corresponding to a country. For ease of exposition, we have stratified countries by the continent they belong to. Note that we have clubbed North and South America together. We may, indeed, expect a rather strong association between these two variables. However, this relationship is complex, with the cloud of points showing a clear C-shape.

A closer investigation by [8] reveals the presence of two possible and opposite effects. First, an “decreasing” effect, from “moderate” birth rate to “low” birth rate as death rate increases, for the industrialized countries (mostly Europe, Oceania and the Americas); and second, an “increasing” effect, from “moderate” birth rate to “high” birth rate as death rate increases, mostly for African nations. The trend is more pronounced for the decreasing effect, while the increasing effect is more diffused.

The strength of this nonlinear structure of dependence is hardly captured by Pearson’s correlation ($\hat{\rho} = -0.125$, not significant at level $\alpha = 0.05$). On the other hand, both `fastMI` ($= 0.333$) and `JMI` ($= 0.451$) detect significant association at level $\alpha = 0.05$.

We further note the disparity between estimated values of MI using both estimators. Since our simulation studies in [subsection 4.1](#) reveal that `fastMI` estimates MI with reduced estimation error, we claim that the JMI overstates strength of association in the data cloud, when compared with `fastMI`. This may lead to erroneous inference in other applications. This example illustrates the benefit of using `fastMI` as a meaningful measure of dependence able to capture nonlinear relationships.

6. Discussion

In this paper we present a fast and consistent MI estimator based on nonparametric copulas. Through extensive simulation studies we have demonstrated that the method has several desirable features of a high-performance MI estimator, outperforming the current gold-standard, the JMI. The method is nonparametric, which means that assumptions about relationships in the data are not imposed. Second, the method is not sensitive to marginal distributions; rather, by virtue of its focus on the copula, it only takes into account the joint association between variables without suffering from potential irregularities in the marginal distribution. We overcome issues that plague bandwidth-based MI estimators, such as bandwidth selection and slow computation times for large data sets. `fastMI` relies on a data-adaptive Fast Fourier transformation-based approach to estimating underlying copula structures. Its run time is many fold faster than the JMI for large data sets. `fastMI` exhibits reduced estimation error and provides a more powerful test of independence than JMI. Finally, using a novel data-splitting approach we present asymptotic theory that allows us to provide confidence intervals associated with MI and perform statistical inference.

Of note, while in this paper we present theory and applications for the bivariate case, `fastMI` is equally applicable to multivariate structures. In brief, we may consider a p -dimensional random vector \mathbf{X} with joint distribution (density) function $F_X (f_X)$ with marginal distribution (density) functions $\{F_i\}_{i=1}^p$ ($\{f_i\}_{i=1}^p$), we can write the unique associated copula density as

$$c(u_1, \dots, u_p) = \frac{f_X(F_1^{-1}(u_1), \dots, F_p^{-1}(u_p))}{\prod_{i=1}^p f_i(F_i^{-1}(u_i))},$$

which may be used to estimate `fastMI` by proceeding in the manner described in [Equation 1](#) and [Equation 2](#). Needless to say, estimation accuracy and rate of convergence of `fastMI` will be adversely affected in higher dimensions.

Due to its adaptability to complex associations and robustness to sample size, `fastMI` will be generally

applicable in a wide range of fields and will advance and enhance the impact of information theory in many domains. Investigations of biological problems in which data collection is constrained by insurmountable practical reasons and is both limited by the difficulty of estimating information accurately from limited samples and by the presence of complex non-linearities [24] will be of particular interest.

To encourage broader dissemination of our proposed toolkit for estimation and testing purposes, we have developed an R package `fastMI` that is publicly available. We attribute the good performance of `fastMI` to two factors: (i) the definition of MI itself and (ii) our estimation method that enjoys several computational and theoretical advantages mentioned above.

7. Technical details

Note that we use `fastMI` and \widehat{MI}_{fast} interchangeably in this section.

7.1. The optimal data-driven kernel

In this section we derive the optimal kernel estimation method associated with the estimate given in (6) of the main article, where “optimal” is intended as minimising the mean integrated square error (*MISE*) between the true density f and its estimator \hat{f} , given by

$$MISE(\hat{f}, f) = \mathbb{E} \left[\int_{\mathbb{R}^2} \{\hat{f}(\mathbf{x}) - f(\mathbf{x})\}^2 d\mathbf{x} \right], \quad (10)$$

where the \mathbb{E} operator denotes taking expectation over the entire support of f . Here we consider density for a continuous random vector. We assume that both the true density f and the kernel density estimate \hat{f} belong to the Hilbert space of square integrable functions (denoted by $\mathcal{L}^2 = \{f : \int f^2(\mathbf{x})d\mathbf{x} < \infty\}$). Originally presented in [33], this section builds on the framework of self-consistent density estimation discussed in [1] and [19].

7.1.1. Preparation

Let us consider a random sample of n_1 observations denoted by $\mathcal{S} = \{\mathbf{Z}_j : (X_j, Y_j) \in \mathcal{Z} = \mathcal{X} \times \mathcal{Y} \subseteq \mathbb{R}^2, j = 1, 2, \dots, n_1\}$, from density f . Without loss of generality, let the sample space $\mathcal{Z} = \mathbb{R}^2$. We consider a generic bivariate kernel density estimator $\hat{f}(\mathbf{x})$ (to be evaluated at any $\mathbf{x} \in \mathcal{X}$) based on a kernel function $K(\mathbf{x})$ which is symmetric with respect to $\mathbf{x} = \mathbf{0}$ and satisfies $\int K(\mathbf{x})d\mathbf{x} = 1$. Specifically, $\hat{f}(\mathbf{x})$ is given by

the convolution of kernel K and the set of delta functions centered on the dataset,

$$\hat{f}(\mathbf{x}) = \frac{1}{n_1} \sum_{j=1}^{n_1} K(\mathbf{z} - \mathbf{Z}_j) = \frac{1}{n_1} \sum_{j=1}^{n_1} \int_{\mathcal{Z}} K(s) \delta(\mathbf{z} - \mathbf{Z}_j - \mathbf{t}) dt, \quad (11)$$

where $\delta(\mathbf{x})$ is the Dirac delta function [15]. Here $\delta(\mathbf{x})$ has the value zero everywhere except at $\mathbf{x} = \mathbf{0}$, where it is a spike of indeterminate magnitude:

$$\delta(\mathbf{x}) = \begin{cases} \rightarrow \infty, & \text{if } \mathbf{x} = \mathbf{0}, \\ 0, & \text{if } \mathbf{x} \neq \mathbf{0}; \end{cases}$$

and it is constrained to have an integral equal to unity $\int_{\mathbb{R}^2} \delta(\mathbf{x}) d\mathbf{x} = 1$. Intuitively, $\delta(\mathbf{x})$ may be viewed as the limit of a multivariate normal distribution as all elements of the covariance matrix approach zero.

Note that in this paper, barring some mild restrictions, the shape of the kernel K is not prefixed, but rather will be determined by a data-driven approach. Further, note that the kernel estimate given by Equation 11 does not depend on any bandwidth matrix \mathbf{H} . This is contrary to the traditional kernel density estimator with a preset kernel function given by

$$\hat{f}_{\mathbf{H}}(\mathbf{z}) = \frac{1}{n_1} \sum_{j=1}^{n_1} K_{\mathbf{H}}(\mathbf{z} - \mathbf{Z}_j), \quad \mathbf{z} \in \mathcal{Z},$$

where \mathbf{H} is a 2×2 bandwidth (or smoothing) matrix which is symmetric and positive definite, the prefixed kernel function K is a symmetric multivariate density, and $K_{\mathbf{H}}(\mathbf{z}) = |\mathbf{H}|^{-1/2} K(\mathbf{H}^{-1/2} \mathbf{z})$ ($|\mathbf{H}|$ denotes the determinant of \mathbf{H}). Standard kernel density estimation techniques involve first choosing, in advance, a certain shape for the kernel K and then searching for an optimal bandwidth \mathbf{H} [26] by a tuning method such as cross validation. Popular choices for the function K include the Epanechnikov kernel K_E given by

$$K_E(\mathbf{x}) \propto (1 - \mathbf{x}'\mathbf{x}) \mathbb{I}(\mathbf{x}'\mathbf{x} \leq 1), \quad \mathbf{x} \in \mathbb{R}^2,$$

where \mathbf{x}' denotes the transpose of a vector \mathbf{x} and the indicator function $\mathbb{I}(\mathbf{x}'\mathbf{x} \leq 1)$ equals unity if $\mathbf{x}'\mathbf{x} \leq 1$ and zero otherwise. Another popular choice is the Gaussian kernel K_G given by

$$K_G(\mathbf{x}) \propto \exp\left(-\frac{\mathbf{x}'\mathbf{x}}{2}\right), \quad \mathbf{x} \in \mathbb{R}^2.$$

See more details in [31].

7.1.2. Derivation of the Fourier transform-based optimal kernel.

Diverging from the classical kernel estimation approach presented by [26], in this paper we focus on obtaining the optimal shape of the kernel K directly. Thus our aim is to obtain \hat{K} - the estimated optimal kernel which minimises the *MISE* of \hat{f} given by Equation 6. To do so, we invoke the Wiener filter-based procedure for signal deconvolution [34] via the following Fourier transform of the unknown density f , denoted by ϕ :

$$\phi(\mathbf{t}) = \mathbb{E} \{ \exp(i\mathbf{t}'\mathbf{X}) \} = \int_{\mathcal{X}} \exp(i\mathbf{t}'\mathbf{x}) f(\mathbf{x}) d\mathbf{x}, \quad \mathbf{t} \in \mathbb{R}^2.$$

We denote the Fourier transform of the estimate \hat{f} by $\hat{\phi}$ and the Fourier transform of the unknown kernel K by κ . Given the estimated optimal transform kernel $\hat{\kappa}$, we may apply the convolution theorem [12] to Equation 11 and obtain $\hat{\phi}(\mathbf{t}) = \hat{\kappa}(\mathbf{t})C(\mathbf{t})$, where C is the (known) empirical characteristic function (ECF) given by

$$C(\mathbf{t}) = \frac{1}{n_1} \sum_{j=1}^{n_1} \exp(i\mathbf{t}'\mathbf{X}_j), \quad \mathbf{t} \in \mathbb{R}^2.$$

Note that the *MISE* in Equation 6 corresponds to the mean-squared distance between the true density f and an estimate \hat{f} , in terms of the Euclidean metric in the Hilbert space of square integrable functions \mathcal{L}^2 (provided $f, \hat{f}, \phi, \hat{\phi} \in \mathcal{L}^2$). Applying Parseval's theorem [12] to rewrite the *MISE* in the Fourier space, we get

$$MISE(\hat{f}, f) = \frac{1}{(2\pi)^2} \mathbb{E} \left(\int_{\mathbb{R}^2} |\hat{\phi}(\mathbf{t}) - \phi(\mathbf{t})|^2 d\mathbf{t} \right). \quad (12)$$

Since the data are independent and identically distributed, according to [30], we have the first two moments of $C(\mathbf{t})$:

$$\mathbb{E} \{ C(\mathbf{t}) \} = \phi(\mathbf{t}), \quad \mathbb{V} (|C(\mathbf{t})|) = (1 - |\phi(\mathbf{t})|^2) / n_1, \quad \mathbf{t} \in \mathbb{R}^2.$$

Together, they yield $\mathbb{E} (|C(\mathbf{t})|^2) = |\phi(\mathbf{t})|^2 + (1 - |\phi(\mathbf{t})|^2) / n_1$. The \mathbb{E} and \mathbb{V} operator denote taking expectation and variance over the entire support of f . Note for any complex number $z = a + ib$, the Euclidean norm is given by $|z| = \sqrt{a^2 + b^2}$. We assume validity of interchanging the integral and expectation operators, and rewrite Equation 12 as follows:

$$MISE(\hat{f}, f) = \frac{1}{(2\pi)^2} \int_{\mathbb{R}^2} \{ (n_1)^{-1} |\kappa(\mathbf{t})|^2 (1 - |\phi(\mathbf{t})|^2) + |\phi(\mathbf{t})|^2 |1 - \kappa(\mathbf{t})|^2 \} d\mathbf{t}. \quad (13)$$

Since f is a PDF, we have $|\phi(\mathbf{t})| \leq 1 \forall \mathbf{t} \in \mathbb{R}^2$, implying non-negativity of the first term in Equation 13, which corresponds to the finite sample size error. Note that the second term does not depend on sample size n_1 . According to nomenclature introduced by [26], these two sources of error are known as the error variance (inversely proportional to n_1) and squared error bias, respectively. Since Equation 13 is quadratic in κ , we may obtain its global minimum by equating the functional derivative of *MISE* with respect to κ to zero, and then solving for the optimal Fourier-transformed kernel κ_{OPT} , which takes the form

$$\kappa_{OPT}(\mathbf{t}) = \frac{n_1}{n_1 - 1 + |\phi(\mathbf{t})|^2}, \quad \mathbf{t} \in \mathbb{R}^2. \quad (14)$$

Using the expression for the transformed optimal kernel in Equation 14 and the convolution theorem [12], we obtain the optimal $\hat{\phi}$ given by

$$\hat{\phi}(\mathbf{t}) = \hat{\kappa}(\mathbf{t})C(\mathbf{t}) = \frac{n_1 C(\mathbf{t})}{n_1 - 1 + |\phi(\mathbf{t})|^2}, \quad \mathbf{t} \in \mathbb{R}^2, \quad (15)$$

where $\hat{\phi}$ may be recognised as the Fourier transform of the optimal density estimate \hat{f} . Equation 15 implies that for each $\mathbf{t} \in \mathbb{R}^2$,

$$\hat{\phi}(\mathbf{t}) \xrightarrow{a.s.} \phi(\mathbf{t}),$$

because $C(\mathbf{t}) \rightarrow \phi(\mathbf{t})$ and $|\phi(\mathbf{t})| \leq 1$. Intuitively this implies that while an infinite sample would reproduce the true density itself, for finite n_1 , the optimal estimate $\hat{\phi}$ downweights the frequencies that contribute less to the estimator of the true density - this procedure may be compared to smoothing.

7.1.3. Iterative procedure to obtain $\hat{\phi}$.

We implement an iterative procedure based on Equation 15 to obtain $\hat{\phi}(\mathbf{t})$ for a given sample of size n_1 , which requires a starting value $\hat{\phi}_0(\mathbf{t})$. The updating rule at the r -th step is given as follows:

$$\hat{\phi}_{r+1}(\mathbf{t}) = \frac{n_1 C(\mathbf{t})}{n_1 - 1 + |\hat{\phi}_r(\mathbf{t})|^2}, \quad r = 0, 1, \dots \quad (16)$$

$\hat{\phi}$ is obtained as the fixed point of the iteration described in Equation 16, and at convergence, the resulting estimator is denoted by $\hat{\phi}$. Having obtained $\hat{\phi}$, we can use the Fourier anti-transformation of the following form:

$$\hat{f}(\mathbf{x}) = \frac{1}{(2\pi)^2} \int_{\mathbb{R}^2} \exp(-i\mathbf{t}'\mathbf{x}) \hat{\phi}(\mathbf{t}) d\mathbf{t} \quad (17)$$

to obtain the optimal density estimate \hat{f} . Also, upon convergence of the iterative procedure, the solution $\hat{\phi}$ satisfies the quadratic equation $(n_1 - 1)|\hat{\phi}(\mathbf{t})|^2 + 1 = n_1|\hat{\phi}(\mathbf{t})||C(\mathbf{t})|$. Solving for $\hat{\phi}$, we follow [1] to choose the following non-null solution:

$$\hat{\phi}(\mathbf{t}) = \frac{n_1 C(\mathbf{t})}{2(n_1 - 1)} \left[1 + \sqrt{1 - \frac{4(n_1 - 1)}{|n_1 C(\mathbf{t})|^2}} \right] \mathbb{I}_{A_{n_1}}(\mathbf{t}), \quad (18)$$

which is regarded as the stable solution, where A_{n_1} serves as a low-pass filter that ensures stability of the estimation process.

Remark 1. *The purpose of the filter $\mathbb{I}_{A_{n_1}}(\mathbf{t})$ is to define a Fourier-based low-pass filter on the ECF $C(\mathbf{t})$ that yields a stable optimal estimate in the minimum MISE sense. Primarily, the set A_{n_1} is specified such that:*

$$A_{n_1} = \left\{ \mathbf{t} \in \mathbb{R}^2 : |C(\mathbf{t})|^2 \geq C_{\min}^2 = \frac{4(n_1 - 1)}{n_1^2} \right\}. \quad (19)$$

Here, the primary filter is necessary in Equation 18 for stability of the estimation method because the lower bound C_{\min} can ensure a well-defined square root term in Equation 18 for $\hat{\phi}$. Moreover, according to [1], the set A_{n_1} may exclude an additional small subset of frequencies to produce a smoother density estimate \hat{f} . In order for \hat{f} to converge to the true density f as n_1 increases, we require that this set of additionally excluded frequencies must shrink, so that the set A_{n_1} of included frequencies grows with increasing n_1 .

Remark 2. *According to [19], the multidimensional ECF $C(\mathbf{t})$ consists of a finite set of contiguous hypervolumes denoted by $\{HV_l^{n_1}\}_{l=1}^{k_{n_1}}$, where k_{n_1} is a finite integer. Each hypervolume permits “above-threshold” frequency values \mathbf{t} for which the constraint in Equation 19 holds. Note that at least one such contiguous hypervolume containing $\mathbf{t} = \mathbf{0}$ is guaranteed to exist since $C(\mathbf{0}) = 1$ due to normalisation and the primary filter A_{n_1} has a lower bound $C_{\min} \leq 1$. Following the suggestion by [19] we employ the lowest contiguous hypervolume filter, choosing the only hypervolume centered at $\mathbf{t} = \mathbf{0}$, which we denote as $HV_1^{n_1}$ for notational convenience. We make the following observations about $HV_1^{n_1}$:*

1. *The set of frequencies included in the lowest contiguous hypervolume filter are bounded above since they will always be contained within a finite-sized hypervolume around the origin.*
2. *The volume of the lowest contiguous hypervolume filter grows as the number of data points n_1 increases, implying more frequencies are included for larger sample sizes.*

The resulting filter satisfies the convergence conditions described by [1]. Hence, we set $A_{n_1} = HV_1^{n_1}$,

and study convergence of \hat{f} to the true f as n_1 increases. For notational convenience, let \bar{A}_{n_1} denote the complement set of A_{n_1} and $\mathcal{V}(A_{n_1})$ denote the volume of A_{n_1} .

7.1.4. Large sample behaviour of the optimal density estimator.

In this section we prove [Theorem 3](#) which establishes strong consistency of the estimator \hat{f} to the true density f as $n_1 \rightarrow \infty$ at all points on the support of f .

Theorem 3. *Let the true density f be square integrable and its corresponding Fourier transform ϕ be integrable. Under the assumptions $\mathcal{V}(A_{n_1}) \rightarrow \infty$, $\mathcal{V}(A_{n_1})/\sqrt{n_1} \rightarrow 0$ and $\mathcal{V}(\bar{A}_{n_1}) \rightarrow 0$ as $n \rightarrow \infty$, we have the estimate \hat{f} , as defined by [Equation 17](#), converging almost surely to the true density f as $n_1 \rightarrow \infty$.*

Note the frequency filter A_{n_1} , its complement \bar{A}_{n_1} and its volume $\mathcal{V}(A_{n_1})$ are described in [Remarks 1](#) and [2](#). Since the true density f and the estimator \hat{f} are both square-integrable, we can express them in terms of their corresponding Fourier transforms ϕ and $\hat{\phi}$ respectively. Since the characteristic function is integrable, we have, $\int |\phi(\mathbf{t})| d\mathbf{t} < \infty$. Through the following sequence of inequalities, we are able to establish an upper bound for the absolute error $|\hat{f}(\mathbf{x}) - f(\mathbf{x})|$ for any $\mathbf{x} \in \mathcal{X}$. By definition, note that $\hat{\phi}(\mathbf{t}) = 0$ for $\mathbf{t} \notin A_{n_1}$. To establish [Theorem 3](#), it is sufficient to show that the upper bound of the absolute error given below tends to zero as $n_1 \rightarrow \infty$. We have:

$$\begin{aligned}
|\hat{f}(\mathbf{x}) - f(\mathbf{x})| &= \left| \frac{1}{(2\pi)^2} \int_{\mathbb{R}^2} \exp(-i\mathbf{t}'\mathbf{x}) \{\hat{\phi}(\mathbf{t}) - \phi(\mathbf{t})\} d\mathbf{t} \right| \\
&\leq \frac{1}{(2\pi)^2} \int_{\mathbb{R}^2} |\exp(-i\mathbf{t}'\mathbf{x})| |\hat{\phi}(\mathbf{t}) - \phi(\mathbf{t})| d\mathbf{t} = \frac{1}{(2\pi)^2} \int_{\mathbb{R}^2} |\hat{\phi}(\mathbf{t}) - \phi(\mathbf{t})| d\mathbf{t} \\
&= \frac{1}{(2\pi)^2} \int_{A_{n_1}} |\hat{\phi}(\mathbf{t}) - \phi(\mathbf{t})| d\mathbf{t} + \frac{1}{(2\pi)^2} \int_{\bar{A}_{n_1}} |\phi(\mathbf{t})| d\mathbf{t} \\
&\leq \frac{1}{(2\pi)^2} \int_{A_{n_1}} |\hat{\phi}(\mathbf{t}) - C(\mathbf{t})| d\mathbf{t} + \frac{1}{(2\pi)^2} \int_{A_{n_1}} |C(\mathbf{t}) - \phi(\mathbf{t})| d\mathbf{t} + \frac{1}{(2\pi)^2} \int_{\bar{A}_{n_1}} |\phi(\mathbf{t})| d\mathbf{t} \\
&:= D_1 + D_2 + D_3.
\end{aligned} \tag{20}$$

Under the assumptions, $\lim_{n_1 \rightarrow \infty} \mathcal{V}(A_{n_1}) = \infty$ and $\lim_{n_1 \rightarrow \infty} \mathcal{V}(\bar{A}_{n_1}) = 0$. Consequently, the second term in [Equation 20](#), $D_2 \rightarrow 0$ as $n_1 \rightarrow \infty$ due to [Theorem 1](#) of [\[4\]](#). Further, $D_3 \leq \mathcal{V}(\bar{A}_{n_1})/(2\pi)^2$, since $|\phi(\mathbf{t})| \leq 1$. Consequently, $D_3 \rightarrow 0$ as $n_1 \rightarrow \infty$.

To prove $D_1 \rightarrow 0$ as $n_1 \rightarrow \infty$, we first consider the two following disjoint sets,

$$\begin{aligned} B_{n_1}^+ &= \{t : |C(t)|^2 \geq 4(n_1 - 1)/n_1^2\}, \\ B_{n_1}^- &= \{t : |C(t)|^2 < 4(n_1 - 1)/n_1^2\}. \end{aligned}$$

Using Equation [Equation 18](#), we rewrite the first integral D_1 as follows

$$\begin{aligned} D_1 &= \frac{1}{2\pi} \int_{A_{n_1} \cap B_{n_1}^+} |C(t)| \left(1 - \frac{n_1}{2(n_1 - 1)} \left[1 + \sqrt{1 - \frac{4(n_1 - 1)}{|n_1 C(t)|^2}} \right] dt \right) + \frac{1}{2\pi} \int_{A_{n_1} \cap B_{n_1}^-} |C(t)| dt \\ &:= D_4 + D_5. \end{aligned}$$

The first term D_4 may be simplified by noting that for $t \in B_{n_1}^+$, we have $|C(t)|^2 \geq 4(n_1 - 1)/n_1^2$. This ensures a non-negative argument under the square root operation. Using the inequality $\sqrt{1-x} + \sqrt{x} \geq 1$ for $0 \leq x \leq 1$ for D_4 , and using the inequality

$$|C(t)| \leq \sqrt{4(n_1 - 1)/n_1^2} \text{ for } t \in B_{n_1}^-,$$

we establish that D_1 is bounded as follows:

$$\begin{aligned} D_1 &= D_4 + D_5 \\ &\leq \frac{1}{(2\pi)^2} \int_{A_{n_1} \cap B_{n_1}^+} \left\{ \frac{1}{\sqrt{n_1 - 1}} - \frac{|C(t)|}{n_1 - 1} \right\} dt + \frac{\sqrt{4(n_1 - 1)}}{n_1(2\pi)^2} \int_{A_{n_1} \cap B_{n_1}^-} dt \\ &\leq \frac{1}{(2\pi)^2} \left\{ \frac{1}{\sqrt{n_1 - 1}} + \frac{1}{n_1 - 1} \right\} \int_{A_{n_1} \cap B_{n_1}^+} dt + \frac{\sqrt{4(n_1 - 1)}}{n_1(2\pi)^2} \int_{A_{n_1}} dt \\ &= \frac{1}{(2\pi)^2} \left\{ \frac{1}{\sqrt{n_1 - 1}} + \frac{1}{n_1 - 1} \right\} \mathcal{V}(A_{n_1} \cap B_{n_1}^+) + \frac{\sqrt{4(n_1 - 1)}}{n_1(2\pi)^2} \mathcal{V}(A_{n_1} \cap B_{n_1}^-) \\ &\leq \frac{1}{(2\pi)^2} \left\{ \frac{1}{\sqrt{n_1 - 1}} + \frac{1}{n_1 - 1} + \frac{\sqrt{4(n_1 - 1)}}{n_1} \right\} \mathcal{V}(A_{n_1}) \\ &\leq \frac{1}{(2\pi)^2} \left\{ \frac{1}{\sqrt{n_1 - 1}} + \frac{1}{n_1 - 1} + \frac{2}{\sqrt{n_1 - 1}} \right\} \mathcal{V}(A_{n_1}). \end{aligned} \tag{21}$$

The assumptions in [Theorem 3](#) include $\mathcal{V}(A_{n_1})/\sqrt{n_1} \rightarrow 0$ as $n_1 \rightarrow \infty$, which ensures that the upper bound in [Equation 21](#) tends to zero for large n_1 . In summary, assuming $\mathcal{V}(A_{n_1}) \rightarrow \infty$, $\mathcal{V}(\bar{A}_{n_1}) \rightarrow 0$, and $\mathcal{V}(A_{n_1})/\sqrt{n_1} \rightarrow 0$ as $n_1 \rightarrow \infty$, we have $|\hat{f}(x) - f(x)| \rightarrow 0$ for every $x \in \mathcal{X}$.

7.2. Consistency of \widehat{MI}_{fast}

Theorem 4. *Let the assumptions of Theorem 3 hold. Further, we assume the true underlying copula function c_{XY} is continuous and bounded away from zero and infinity on its support. Then, the estimator \widehat{MI}_{fast} converges in probability to the true MI as $n \rightarrow \infty$.*

From Theorem 3 we know that for any small ϵ , there exists a large enough N such that $\sup_z |\hat{c}(z) - c(z)| < \epsilon$. Using Taylor series expansion to $\log \{\hat{c}(z_i)/c(z_i)\}$, we get $\log \{\hat{c}(z_i)\} = \log \{c(z_i)\} + \frac{\hat{c}(z_i) - c(z_i)}{c(z_i)} + o(\epsilon)$, where we ignore the last term. Summing the expression above over n observations, we get

$$\begin{aligned} \left| \widehat{MI}_{fast} - MI_{oracle} \right| &= \left| \frac{1}{N} \sum_{i=1}^N \log \{\hat{c}(z_i)\} - \frac{1}{N} \sum_{i=1}^N \log \{c(z_i)\} \right| \\ &\leq \frac{1}{N} \sum_{i=1}^n \left| \frac{\hat{c}(z_i) - c(z_i)}{c(z_i)} \right| \leq \frac{\sup_i |\hat{c}(z_i) - c(z_i)|}{C} < \frac{\epsilon}{C}. \end{aligned}$$

Hence, as MI_{oracle} is consistent for MI, we can claim \widehat{MI}_{fast} is consistent for MI as well.

Acknowledgments

Song's research is partially supported by a NSF Grant DMS2113564.

References

- [1] A. Bernacchia, S. Pigolotti, Self-consistent method for density estimation, *Journal of the Royal Statistical Society: Series B (Statistical Methodology)* 73 (2011) 407–422.
- [2] M. Bolbolian Ghalibaf, Relationship between kendall's tau correlation and mutual information, *Revista Colombiana de Estadística* 43 (2020) 3–20.
- [3] T. M. Cover, J. A. Thomas, *Elements of Information Theory*, Wiley, 2005.
- [4] S. Csörgő, V. Totik, On how long interval is the empirical characteristic function uniformly consistent?, *Acta Sci. Math. (Szeged)* 45 (1983) 141–149.
- [5] C. Czado, *Analyzing Dependent Data with Vine Copulas: A Practical Guide With R (Lecture Notes in Statistics, 222)*, Springer, paperback edition, 2019.
- [6] C. O. Daub, R. Steuer, J. Selbig, S. Kloska, *BMC Bioinformatics* 5 (2004) 118.
- [7] B. S. Everitt, A. Skrondal, *The Cambridge dictionary of statistics*, Cambridge University Press, Cambridge, England, 4 edition, 2010.
- [8] G. Geenens, P. L. de Micheaux, The hellinger correlation, *Journal of the American Statistical Association* 117 (2020) 639–653.

- [9] N.-B. Heidenreich, A. Schindler, S. Sperlich, Bandwidth selection for kernel density estimation: a review of fully automatic selectors, *AStA Advances in Statistical Analysis* 97 (2013) 403–433.
- [10] R. Heller, Y. Heller, M. Gorfine, A consistent multivariate test of association based on ranks of distances, *Biometrika* 100 (2012) 503–510.
- [11] H. Joe, *Dependence Modeling with Copulas* (Chapman & Hall/CRC Monographs on Statistics and Applied Probability), Chapman and Hall/CRC, hardcover edition, 2014.
- [12] D. W. Kammler, *A First Course in Fourier Analysis*, Cambridge University Press, 2008.
- [13] J. B. Kinney, G. S. Atwal, Equitability, mutual information, and the maximal information coefficient, *Proceedings of the National Academy of Sciences* 111 (2014) 3354–3359.
- [14] A. Kraskov, H. Stögbauer, P. Grassberger, Estimating mutual information, *Physical Review E* 69 (2004).
- [15] E. Kreyszig, *Advanced Engineering Mathematics*, Wiley, loose leaf edition, 2020.
- [16] J. Ma, Z. Sun, Mutual information is copula entropy, *Tsinghua Science and Technology* 16 (2008) 51–54.
- [17] B. F. Manly, *Randomization, Bootstrap and Monte Carlo Methods in Biology*, Chapman and Hall/CRC, 2018.
- [18] Y.-I. Moon, B. Rajagopalan, U. Lall, Estimation of mutual information using kernel density estimators, *Phys. Rev. E* 52 (1995) 2318–2321.
- [19] T. A. O’Brien, K. Kashinath, N. R. Cavanaugh, W. D. Collins, J. P. O’Brien, A fast and objective multidimensional kernel density estimation method: fastKDE, *Computational Statistics & Data Analysis* 101 (2016) 148–160.
- [20] L. Paninski, Estimation of entropy and mutual information, *Neural Computation* 15 (2003) 1191–1253.
- [21] A. M. Peter, A. Rangarajan, Maximum likelihood wavelet density estimation with applications to image and shape matching, *IEEE Transactions on Image Processing* 17 (2008) 458–468.
- [22] D. N. Reshef, Y. A. Reshef, H. K. Finucane, S. R. Grossman, G. McVean, P. J. Turnbaugh, E. S. Lander, M. Mitzenmacher, P. C. Sabeti, Detecting novel associations in large data sets, *Science* 334 (2011) 1518–1524.
- [23] C. P. Robert, *Monte Carlo Statistical Methods* (Springer Texts in Statistics), Springer, paperback edition, 2010.
- [24] H. Safaai, A. Onken, C. D. Harvey, S. Panzeri, Information estimation using nonparametric copulas, *Physical Review E* 98 (2018).
- [25] C. E. Shannon, A mathematical theory of communication, *Bell System Technical Journal* 27 (1948) 379–423.
- [26] B. W. Silverman, *Density Estimation for Statistics and Data Analysis*, Chapman I& Hall, London, 1986.
- [27] T. Speed, A correlation for the 21st century, *Science* 334 (2011) 1502–1503.
- [28] S. P. Strong, R. Koberle, R. R. de Ruyter van Steveninck, W. Bialek, Entropy and information in neural spike trains, *Phys. Rev. Lett.* 80 (1998) 197–200.
- [29] G. J. Székely, M. L. Rizzo, N. K. Bakirov, Measuring and testing dependence by correlation of distances, *The Annals of Statistics* 35 (2007).
- [30] N. G. Ushakov, *Selected Topics in Characteristic Functions*, DE GRUYTER, 1999.
- [31] M. Wand, M. Jones, *Kernel Smoothing* (Chapman & Hall/CRC Monographs on Statistics and Applied Probability), Chapman and Hall/CRC, hardcover edition, 1995.
- [32] Q. Wang, S. R. Kulkarni, S. Verdu, Divergence estimation for multidimensional densities via k -nearest-neighbor distances, *IEEE Transactions on Information Theory* 55 (2009) 2392–2405.
- [33] G. S. Watson, M. R. Leadbetter, On the estimation of the probability density, *The Annals of Mathematical Statistics* 34

(1963) 480–491.

[34] N. Wiener, *Extrapolation, Interpolation, and Smoothing of Stationary Time Series*, The MIT Press, 1964.

[35] X. Zeng, Y. Xia, H. Tong, Jackknife approach to the estimation of mutual information, *Proceedings of the National Academy of Sciences* 115 (2018) 9956–9961.

Comparison of mean squared error (MSE) of competing mutual information (MI) estimation methods for various copula families.

The estimation methods compared here are Fast Fourier Transform–based MI (fastMI) and the jackknifed MI (JMI).

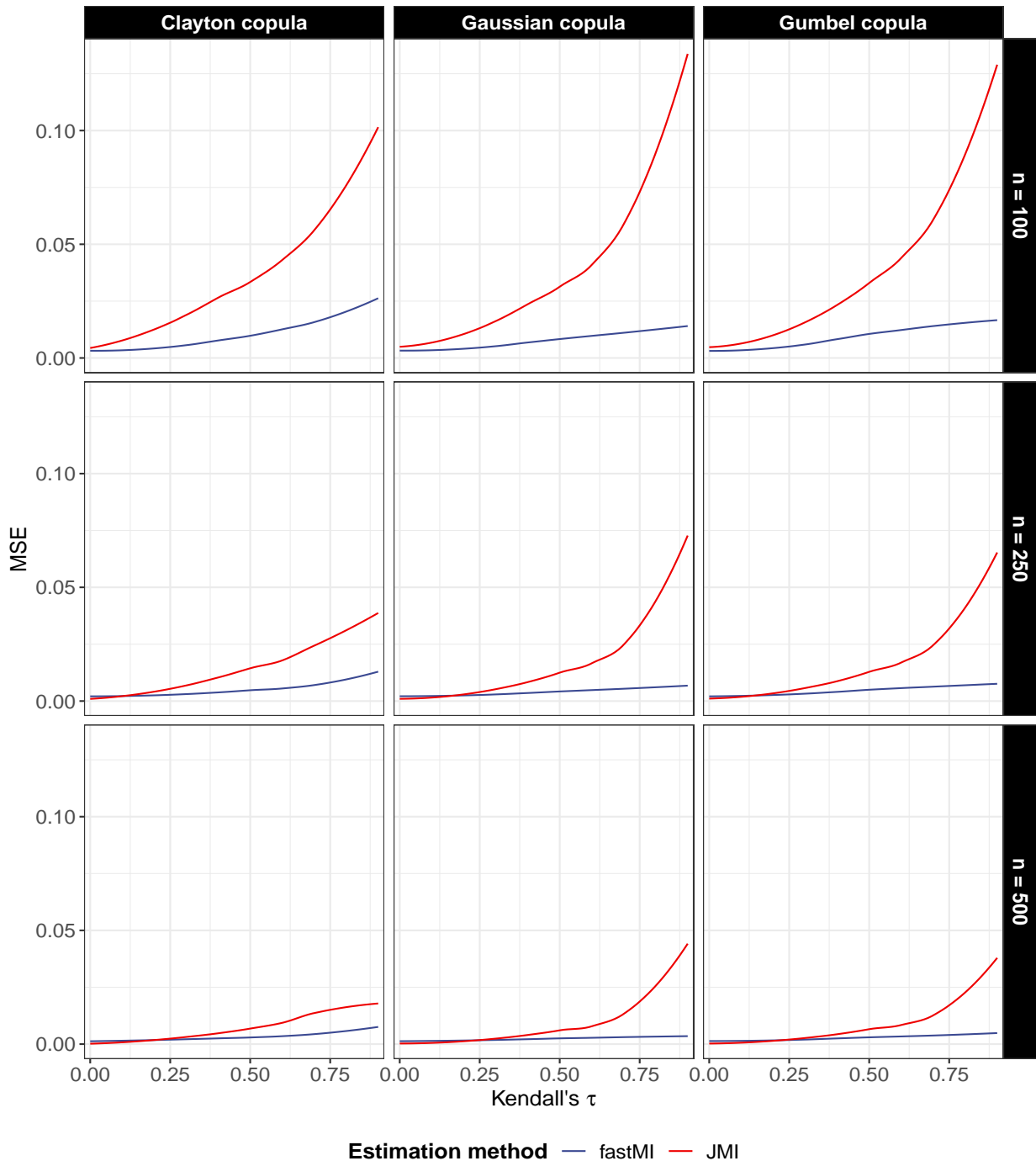


Fig. 1: In each panel, the lines represent mean squared errors (MSE) (y-axis) of different estimation methods based on $r = 1000$ replications for various levels of association controlled by Kendall's τ (x-axis). Correspondence between colors and the methods are as follows: **JMI in red** and **fastMI in blue**.

Comparison of empirical power of competing mutual information (MI) estimation methods for various association patterns.

The estimation methods compared here are Fast Fourier Transform–based MI (fastMI), the jackknifed MI (JMI) and the maximal information coefficient (MIC).

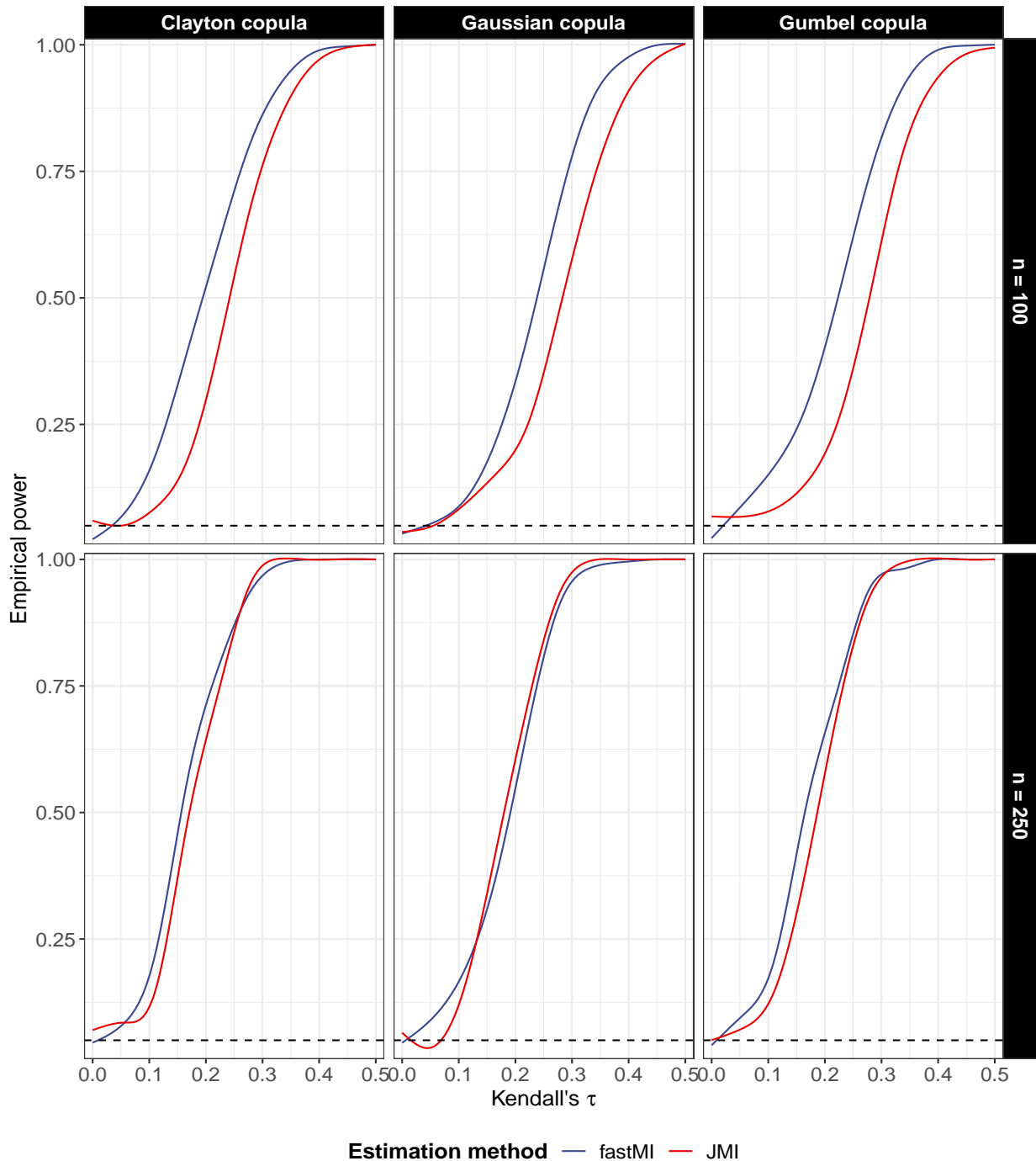


Fig. 2: In each panel, the lines represent the empirical power of tests at significance level $\alpha = 0.05$ for various levels of association controlled by Kendall's τ (x-axis). Dotted line parallel to x-axis denotes $\alpha = 0.05$. Correspondence between colors and the methods are as follows: **JMI in red** and **fastMI in blue**.

Birth rate versus death rate (per thousand individuals) around the world in 2020.

These data are made available in the R package HellCor.
Countries are color-/shape-coded by their continent.

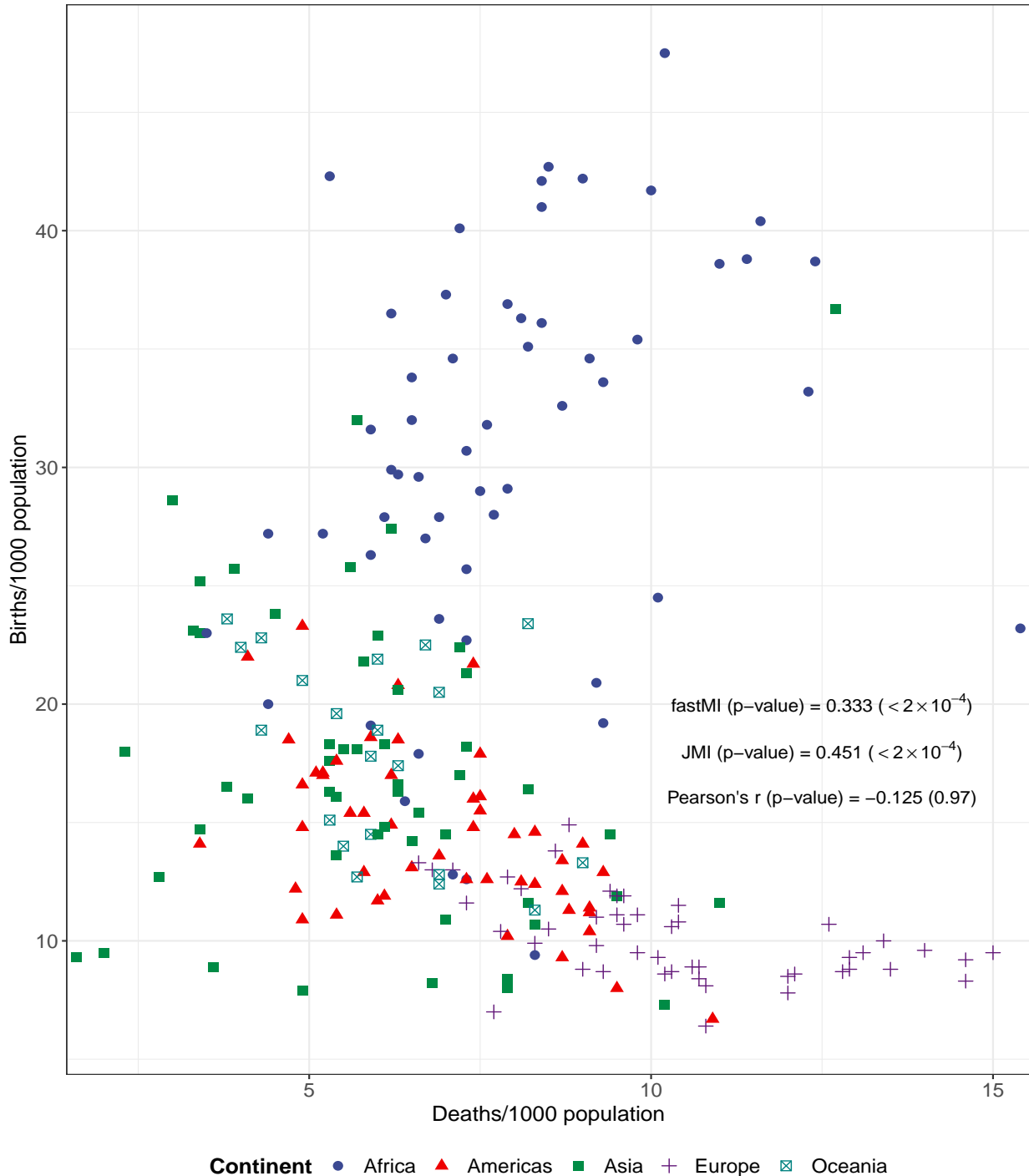


Fig. 3: Association study of birth rate (y-axis) versus death rate (x-axis) in 229 countries and island territories around the world in 2020. These data are made available in the R package HellCor. Countries are stratified by the continent they lie in.